Cancer Chemother Pharmacol (2011) 68:477–487
DOI 10.1007/s00280-010-1504-9

ORIGINAL ARTICLE

Cytotoxic responses to N-(4-hydroxyphenyl)retinamide in human pancreatic cancer cells

Maria C. Messner · Myles C. Cabot

Received: 1 July 2010 / Accepted: 26 October 2010 / Published online: 12 November 2010

Abstract
Purpose Although fenretinide (4-HPR) has been studied in breast cancer and in neuroblastoma, little is known regarding its activity in pancreatic cancer, a neoplasm for which there are few therapeutic options. Since pancreatic cancer cells are susceptible to reactive oxygen species (ROS) and ceramide, two hallmarks of 4-HPR cytotoxicity, we investigated the effect of 4-HPR on human pancreatic cancer cells.
Methods Human pancreatic cancer cell lines MIA PaCa-2 and PANC-1 were treated with 4-HPR, followed by measurement of viability, proliferation, ROS and ceramide production, and Western blotting.
Results At the measured IC_{50} of 10 μM, 4-HPR led to a 44–68% reduction in [^{3}H]thymidine incorporation, a >3-fold increase in de novo ceramide levels, a 2.7-fold increase in ROS, and minor increases in markers of apoptosis. 4-HPR induced a robust, sustained increase in LC3 II expression and enhanced formation of acridine orange–stained acidic vesicles that are markers of autophagy. In addition, sustained, dose-dependent increases in JNK and p38 phosphorylation and decreased ERK phosphorylation were observed following treatment. Pretreatment with vitamin E, a ROS scavenger, and 3-methyladenine, an autophagy inhibitor, individually led to decreased sensitivity to 4-HPR; however, the de novo ceramide inhibitor myriocin had no effect.
Conclusions These data show that 4-HPR triggers pancreatic cancer cell death by apoptosis and autophagy and that sensitivity appears to be mediated by ROS and not ceramide. This study is the first to characterize the response of human pancreatic cancer cells to 4-HPR and opens the door to investigations into this compound in pancreatic adenocarcinomas.

Keywords Fenretinide · 4-HPR · Pancreatic cancer · Reactive oxygen species (ROS) · Autophagy · Ceramide

Abbreviations

4-HPR	N-(4-hydroxyphenyl)retinamide
ROS	reactive oxygen species
3-MA	3-methyladenine
MAPK	mitogen-activated protein kinase
JNK	Jun N-terminal kinase, ERK1/2, extracellular signal-regulated kinase
MTS	3-(4,5-dimethylthiazol-2-yl)-5-(3-carboxymethoxyphenyl)-2-(4-sulfophenyl)-2H-tetrazolium, inner salt
PI	propidium iodide
zVAD	carbobenzoxy-valyl-alanyl-aspartyl-[O-methyl]-fluoromethylketone
dThd	thymidine

Introduction

N-(4-hydroxyphenyl)retinamide (4-HPR), also known as fenretinide, is a synthetic retinoid that has been shown to effectively kill several types of premalignant and malignant tumors, leaving normal cells unharmed [30]. 4-HPR has been used successfully in clinical trials with minimal toxicity for the prevention and treatment of various cancers

M. C. Messner · M. C. Cabot (✉)
Department of Experimental Therapeutics,
John Wayne Cancer Institute, 2200 Santa Monica Blvd,
Santa Monica, CA 90404, USA
e-mail: cabot@jwci.org

including breast [8, 13], prostate [6], head and neck [37], oral leukoplakia [37], and neuroblastoma [34]. A 15-year follow-up study showed that 4-HPR prevented second breast cancer recurrence even after treatment cessation [13]. In the majority of preclinical studies, 4-HPR inhibited proliferation and led to caspase-dependent [2, 20] and caspase-independent apoptosis [16]; however, features of autophagy [12, 33] and necrosis [25] have also been observed.

Pancreatic cancer remains one of the most deadly cancers, as it is largely unresponsive to current surgical and chemotherapies [17]. A review of the literature suggested to us that 4-HPR would likely limit pancreatic cancer cell growth and decrease viability. The ability of 4-HPR to kill cancer cells is multifaceted and has been attributed to increased levels of reactive oxygen species (ROS) and ceramide,[1] activated mitogen-activated protein kinase (MAPK) signaling, and altered Bcl-2 regulation [16]. Recently, it was shown that ceramide regulates gemcitabine-induced cell death in pancreatic cancer cells [26] and that pancreatic cancer cells are particularly sensitive to changes in steady-state respiration and reactive oxygen species (ROS) [10].

In comparison with other carcinomas, there are few studies on pancreatic cancer, although there is a dire need for effective new therapies. 4-HPR is already in clinical trials for the treatment of several cancers [6, 8, 13, 34, 37]; however, 4-HPR has not been studied in pancreatic cancer. Here, we characterize for the first time the effects of clinically relevant concentrations 4-HPR on pancreatic cancer cells.

Materials and methods

Reagents and cell culture

All high-grade reagents were purchased from Sigma (St. Louis, MO) or Fisher (Pittsburg, PA) unless otherwise indicated. The human pancreatic carcinoma cell lines PANC-1 and MIA PaCa-2 were purchased from the American Type Culture Collection (Manassas, VA) and maintained in complete medium, which is RPMI 1640 medium supplemented with 10% FBS (Atlanta Biologicals, Lawrenceville, GA), 100 U/ml penicillin, 100 μg/ml streptomycin, and 100 mM L-glutamine (Invitrogen, Carlsbad). In all experiments, cells were seeded into cultureware and allowed to adhere overnight at 37°C, 5% CO_2. Vitamin E (α-tocopherol) was made fresh in ethanol and added to 1 M HEPES buffer; 3-methyladenine (3-MA) was mixed in water/ethanol (94:6 v/v) and heated to 50°C before use; desipramine was dissolved in water; GW4869 was dissolved in DMSO. Myriocin (Matreya, Pleasant Gap, PA) and 4-HPR (Calbiochem, San Diego) were dissolved in ethanol; fumonisin B1 (Calbiochem, San Diego) was dissolved in DMSO; L-cycloserine (Enzo, Plymouth Meething, PA) was dissolved in water. All reagents were stored at −20°C, and immediately prior to addition to cultured cells, were reconstituted in complete medium containing 5% FBS supplemented with 25 mM HEPES. Pretreatments were for 2 h and were not counted as part of the experimental time point. [^{3}H]Palmitic acid (60–80 Ci/mmol in ethanol) and [^{3}H]thymidine (60–80 Ci/mmol in water) were from American Radiolabeled Chemicals (St. Louis, MO). FACSFlow™ and Z-VAD-FMK (carbobenzoxy-valyl-alanyl-aspartyl-[O-methyl]-fluoromethylketone) were purchased from BD Biosciences (San Jose, Ca); BCA (bicinchoninic acid) protein assay and SuperSignal® West Pico chemiluminescent substrate were purchased from Pierce (Rockford, IL). Carboxy-H_2DCFDA for ROS detection, acridine orange for autophagy detection, precast gels, and electrophoresis and Western blotting buffers were purchased from Invitrogen (Carlsbad, CA). All antibodies were from Cell Signaling Technologies (Danvers, MA). CellTiter 96® AQ_{ueous} (3-(4,5-dimethylthiazol-2-yl)-5-(3-carboxymethoxyphenyl)-2-(4-sulfophenyl)-2H-tetrazolium, inner salt; MTS) and Caspase-Glo® were purchased from Promega (Madison, WI). Sphingolipid standards for TLC (thin-layer chromatography) were purchased from Avanti Polar Lipids (Alabaster, AL).

Sphingolipid analysis

To measure de novo ceramide production, 24 h after seeding 2×10^5 cells into 12-well plates and following 2-h inhibitor pretreatments (0.25 μM myriocin, 25 μM fumonisin B1, 10 mM L-cycloserine, 10 μM desipramine, or 10 μM GW4869), 1 μCi/ml [^{3}H]palmitic acid, and 4-HPR in culture medium were added to cells for 2 or 24 h. To measure ceramide derived from the salvage pathway, cells were pulsed for 24 h with 1 μCi/ml [^{3}H]palmitic acid per well and chased for 2 h with vehicle or inhibitors in fresh medium without [^{3}H]palmitic acid, followed by 10 μM 4-HPR for the indicated times. At the end of the treatment periods, lipids were extracted as described previously [35]. The organic phase was dried under a stream of nitrogen gas, and lipids were reconstituted in chloroform/methanol (2:1 v/v). An aliquot was taken from each sample to determine total lipid radioactivity by liquid scintillation counting. One-fourth or one-fifth of the total lipid extract from each sample was resolved by TLC on layers of Silica Gel G (Analtech, Newark, DE) as previously described [35]. The area of the TLC plate corresponding to standards was scrapped into vials and mixed with 0.5 ml water, followed

[1] "Ceramide" refers to the entire class of ceramide and dihydroceramide molecular species, unless otherwise noted.

by 4 ml Ecolume scintillation fluid (MP Biomedicals, Solon, OH). Radioactivity was measured in a Liquid Scintillation 6500 counter (Beckman Coulter, Brea, CA).

MTS assay

Cells (3,000/well) seeded into 96-well plates were assayed at 72 h by addition of MTS reagent, and color development was analyzed on an FL600 plate reader (BioTek Instruments, Winooksi, VT).

Caspase 3/7 activity

Cells (7,000/well) seeded into 96-well plates were assayed at 6, 24, and 48 h by addition of Caspase-Glo® 3/7 substrate according to the manufacture's instructions, and luminescence was measured on a GloMax® Luminometer (Promega, Madison, WI).

[^{3}H]Thymidine incorporation

PANC-1 (3×10^5/well) seeded into 6-well plates were treated with various agents. One hour prior to the end of treatment, 2 μCi/ml [^{3}H]thymidine was added, and culture plates were placed at 37°C. After 1 h, plates were placed on ice, medium was discarded, and cells were washed with ice-cold PBS. Methanol/acetic acid (3:1 v/v) was added to cells for 5 min and aspirated; methanol/acetic acid wash was repeated twice more. NaOH (1 N) was added to wells, plates were placed in the incubator for 10 min, followed by neutralization with 1 N HCl. The reaction mixtures were collected, and radioactivity was evaluated by liquid scintillation counting.

Microscopy

Cells (2×10^5/well) seeded into 6-well plates were treated with various agents and monitored over time. Following 48-h treatment, cells in culture medium were exposed to the single agent acridine orange (1 μg/ml) for 10 min in the dark. In acridine orange–treated cells illuminated with blue (488 nm) excitation light, the cytosol and nucleolus fluoresce green, RNA fluoresce pale yellow/orange, and acidic compartments, such as autolysosomes, fluoresce bright orange/red. For ROS visualization, cells were washed twice with PBS, carboxy-H_2DCFDA (2.5 μM in PBS) was added to the cells for 10 min in the dark, and cells were allowed to recover in serum-free RPMI 1640 medium in the incubator for 30 min. Photomicrographs were obtained on an Olympus IX70 microscope equipped with a mercury lamp with a 488-nm band-pass blue excitation filter. Images were collected on a Nikon DS-2Mv-UI and processed using NIS Elements F 3.0 software.

Flow cytometry

For ROS determination, cells were washed twice with PBS and exposed to carboxy-H_2DCFDA (2.5 μM) for 10 min at room temperature in the dark. The probe was aspirated off, and cells were allowed to recover in the incubator in serum-free medium for 30 min. Cells were then exposed to EDTA-trypsin, collected in complete medium, centrifuged at 200 g for 5 min at 4°C, and resuspended in PBS. For apoptosis and cell viability determination, cells floating in the medium were collected into tubes; adherent cells were trypsinized and pooled with floating cells. Cells were then centrifuged at 200 g for 5 min at 4°C and washed with PBS. Approximately 10^5 cells were resuspended in binding buffer containing FITC-Annexin V and propidium iodide, or propidium iodide alone (5 μg/ml), according to the manufacture's instructions. Cells (10^4/sample) were processed on a FACSCalibur™ (BD Biosciences, San Jose, CA), and data were analyzed using CellQuest™ software. Debris was excluded by gating on forward and side scatter.

Western blotting

Cells ($2x10^5$) seeded in 35-mm culture dishes were treated with various agents for 12, 24, or 48 h. Cells were washed twice with PBS and lysed on ice in lysis buffer (Tris–HCl (pH 7.4), 1% Triton X-100, 10% glycerol, 0.1% SDS, 1 mM EDTA, 1 mM EGTA, protease inhibitor cocktail, 1 mM NaF, 2 mM Na_3VO_4, and 1 μM phenylmethylsulfonyl fluoride). Cells were scrapped into tubes with rubber policemen and subjected to one freeze–thaw cycle. Lysates were centrifuged at 13,000 rpm for 10 min at 4°C, and supernatants were collected. Protein concentration was determined using BCA reagent, and 50 μg was reconstituted into NuPAGE® 4X LDS sample buffer, β-mercaptoethanol, and water to ensure equal volume loading per lane. Samples were heated to 70°C for 5 min, loaded onto NuPAGE® Bis–Tris 4–12% gradient gels, and SDS–PAGE was performed. Following transfer and block, membranes were incubated with primary antibody in 5% BSA in TBST overnight at 4°C on a shaker. Appropriate horseradish peroxidase–conjugated secondary antibody diluted into TBST/milk was added to membranes for 1 h. Following chemiluminescent substrate incubation, images were collected on a FluorChem® FC2 imaging system using AlphaView® 1.2.1.0 software. Membranes were stripped (100 mM glycine and 0.1% SDS, pH 2.5) and reprobed with β-actin to monitor protein loading. Brightness and contrast were adjusted within the linear range on all images in Adobe® Photoshop®.

Statistics

Data are expressed as mean ± SEM; *n* indicates the number of repeated experiments. A two-tailed Student's *t*-test was performed for comparisons of two means (e.g. the control arm and treatment arm). For multiple comparisons (e.g. the effects of various treatments to control, or between treatments), statistical analysis was performed using a one-way ANOVA followed by Tukey's post hoc test. Differences were considered statistically significant when $P \leq 0.05$. An asterisk (*) denotes significance over the control arm, and a number sign (#) denotes significance over 4-HPR experimental arm.

Results

4-HPR decreases viability and proliferation

Following 4-HPR treatment, a loss of viability/proliferation and an approximate IC_{50} of 10 μM were observed in both pancreatic cancer cell lines (Fig. 1a). It should be noted that a blood serum concentration of 12.9 μM can be achieved in pediatric neuroblastoma patients receiving oral doses of 4-HPR [14]. At 18 h after 4-HPR exposure, DNA synthesis declined to 56% of control in PANC-1 and 32% of control in MIA PaCa-2 (Fig. 1b). PI staining revealed little increase in cell death at 24 h and a >3-fold increase at 72 h (Fig. 1c), suggesting 4-HPR initially decreases proliferation followed by cell death.

Effect of 4-HPR on sphingolipid production

4-HPR has been shown to increase cellular ceramide levels by stimulating de novo ceramide production [36] and inhibiting dihydroceramide desaturase activity [21]. Accordingly, we measured ceramide generated from the de novo pathway and from sphingomyelin by sphingomyelinase. Within 2 h, ceramide generated by the de novo pathway doubled following exposure to 4-HPR (Fig. 2a). At 24 h after 4-HPR exposure, de novo-generated ceramide increased 3.3-fold, with concomitant increases in glucosylceramide (3.9-fold) and sphingomyelin (1.7-fold) (Fig. 2b), indicative of robust anabolic pathways for regulating ceramide levels in these cells. Pulse-chase experiments showed little to no increase in sphingomyelin-derived ceramide in PANC-1 or MIA PaCa-2 cells at 15 min ($P = 0.6$ and 0.38, respectively) nor at 2 h ($P = 0.14$ and 0.446, respectively). Minor but significant increases in ceramide were measured at 6 and 24 h (Fig. 2c); however, GW4869 and desipramine, neutral and acid sphingomyelinase inhibitors, respectively, did not block sphingomyelinase-derived ceramide production (Fig. 2c). GW4869 and desipramine did not block the generation of de novo ceramide as expected (data not shown). The increase in ceramide following 4-HPR treatment was blocked only by de novo ceramide inhibitors myriocin and fumonisin B1, which block serine palmitoyltransferase and ceramide synthase, respectively, and L-cycloserine, which competes for serine at the first step of synthesis (Fig. 2b, c).

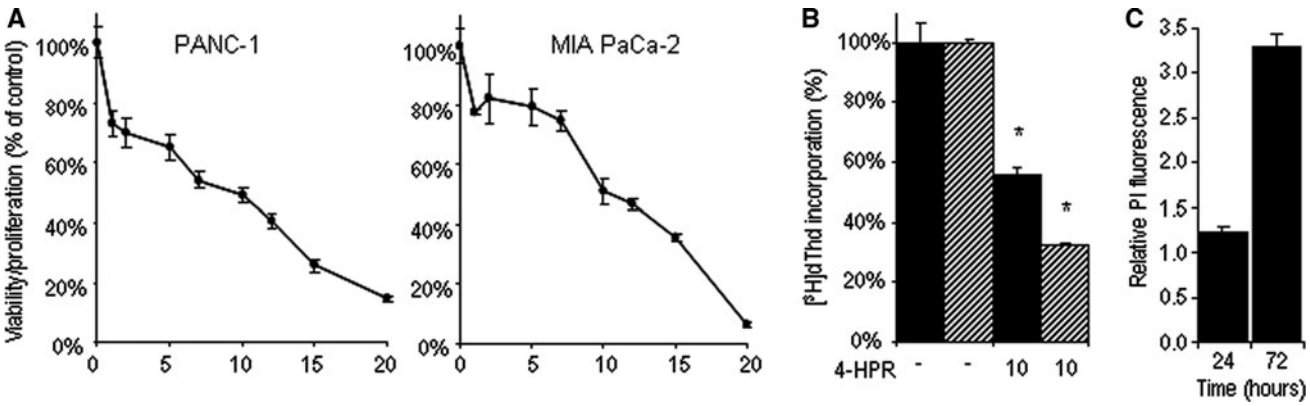

Fig. 1 Effect of 4-HPR on pancreatic cell viability and proliferation. **a** Proliferation/viability assays (MTS) were performed on PANC-1 and MIA PaCa-2 cells after a 72-h exposure to the concentrations of 4-HPR indicated, compared with vehicle control; n = 6. **b** DNA synthesis in PANC-1 (*black bars*) and MIA PaCa-2 (*hatched bars*) was measured after an 18-h treatment with 10 μM 4-HPR or vehicle (−). Cells were then exposed to 2 μCi/ml [^{3}H]thymidine (dThd) for 1 h. The reaction mixtures were collected as detailed in "Materials and methods", and radioactivity was evaluated by liquid scintillation counting. **c** Cell death analyzed by flow cytometry. Cells were treated with vehicle or 10 μM 4-HPR for 24 and 72 h. Cells were stained with propidium iodide (PI) and analyzed by flow cytometry. *Bar graph* shows fold increase in mean PI fluorescence in treated cells compared with control; $n = 3$, error bars show SEM of ratios. An *asterisk* denotes a significant difference between the control arm, $P \leq 0.05$

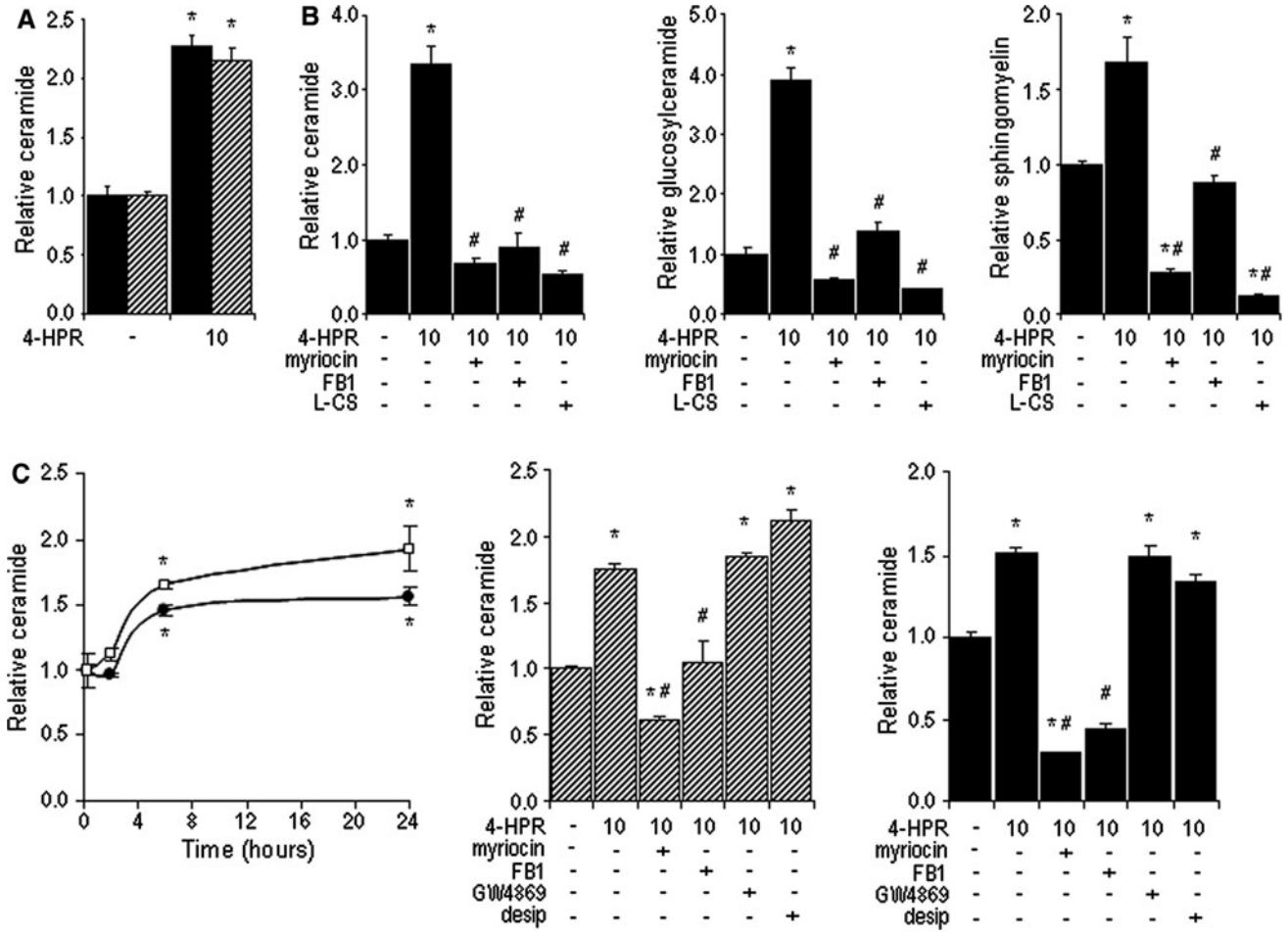

Fig. 2 Effect of 4-HPR on sphingolipid production. **a**, **b** De novo ceramide generation. Cells were pretreated with 0.25 μM myriocin, 25 μM fumonisin B1 (FB1), and 10 mM L-cycloserine (L-CS) for 2 h, followed by treatment with medium containing [^{3}H]palmitic acid and 10 μM 4-HPR or vehicle (−) for (**a**) 2 h or (**b**) 24 h. **c** Sphingomyelinase-generated ceramide. Ceramide derived by the salvage pathway was measured in PANC-1 (*closed circles*) or MIA PaCa-2 cells (*open squares*) by pulsing cells with [^{3}H]palmitic acid for 24 h, a 2-h chase with 10 μM GW4869 or 10 μM desipramine, followed by exposure to vehicle (−) or 10 μM 4-HPR for indicated times. Student's *t*-test was performed ($n = 3$). An *asterisk* denotes a significant difference between the control arm, $P \leq 0.05$. Radiolabeled lipids were analyzed by thin-layer chromatography following total lipid extraction. Ceramide dpm was divided by total lipid dpm for each sample. Data represent fold change over control levels. One-way ANOVA with Tukey's *post hoc* analyses was preformed ($n = 3$). An *asterisk* denotes a significant difference between the control arm, and a number sign denotes a significant difference between the 4-HPR experimental arm, $P \leq 0.05$

4-HPR increases ROS generation

Increased ROS production in cancer cells is a hallmark effect of 4-HPR treatment and a major contributor of 4-HPR-induced cancer cell death [16]. However, not all cancer cells respond to 4-HPR by increased ROS yet are sensitive to 4-HPR-induced cytotoxicity [31]. In both PANC-1 and MIA PaCa-2 cell lines, 4-HPR treatment elicited ROS production in cells, whereas control cells generated little to no ROS (Fig. 3a). Figure 3b demonstrates that ROS production was dose responsive at 24 h and increased over time following 4-HPR exposure. To determine whether ROS induced by 4-HPR exposure contributed to the ceramide increases, PANC-1 cells were pretreated with the antioxidant vitamin E. Blocking ROS did not alter ceramide levels, nor did it attenuate the generation of ceramide in response to 4-HPR (Fig. 3c), suggesting that ROS does not drive the production of de novo ceramide under our experimental conditions.

Effect of 4-HPR on markers of apoptosis

4-HPR treatment led to minor, albeit significant, dose-dependent increases in caspase 3/7 activity (Fig. 4a, b, c), which were attenuated by pretreatment with the pan-caspase inhibitor Z-VAD-FMK (ZVAD) (Fig. 4b,c). The table in Fig. 4d, a compilation of PI and FITC-conjugated Annexin V flow cytometry data, shows that 4-HPR induced

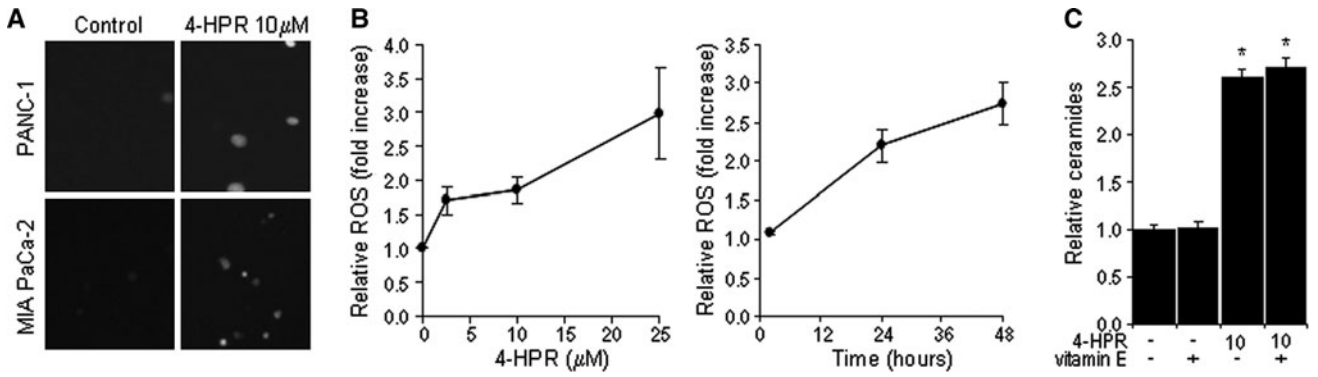

Fig. 3 Effect of 4-HPR on the production of reactive oxygen species. **a** Fluorescence microscopy of carboxy-H_2DCFDA-treated PANC-1 and MIA PaCa-2 cells was performed following 24-h incubation with 10 μM 4-HPR or vehicle (*Control*). **b** Flow cytometry of carboxy-H_2DCFDA-treated PANC-1 was performed following 24-h incubation with 0, 2.5, 10, and 25 μM 4-HPR (graph on *left*), or following a 10 μM 4-HPR incubation for 2, 24, or 48 h (graph on *right*). Data are displayed as fold change over control. **c** Effect of vitamin E on de novo ceramide production. PANC-1 cells were pretreated with 250 μM vitamin E for 2 h, followed by treatment with 10 μM 4-HPR or vehicle (−) for 24 h in medium containing [^{3}H]palmitic acid. Data represent fold change over control levels. One-way ANOVA with Tukey's *post hoc* analyses was preformed ($n = 3$). An *asterisk* denotes a significant difference between the control arm, and a number sign denotes a significant difference between the 4-HPR experimental arm, $P \leq 0.05$

a small, dose-dependent increase in Annexin V/PI-positive cells over control. The percentage of Annexin V/PI-positive cells following 10 μM 4-HPR treatment was diminished by pretreatment with ZVAD. Lastly, little to no cleaved PARP was detected by Western blot (Fig. 4e). Other measures of apoptosis including DNA laddering and differential expression of caspase-independent expression of apoptosis initiator factor (AIF) were not evident (data not shown).

4-HPR treatment elicits autophagy

In response to 4-HPR treatment, large and small red acidic vesicles formed in PANC-1 and MIA PaCa-2 cells, whereas controls did not exhibit red vesicle staining (Fig. 5a). Exposure to 4-HPR also led to a marked increase in LC3 II protein expression in MIA PaCa-2 (Fig. 5b) and in PANC-1 cells (Fig. 5c). LC3 II expression was similar to control levels at 12 h, but expression was elevated at 24 and 48 h (Fig. 5b, c). Pre-incubation with autophagy inhibitor 3-MA or ROS inhibitor vitamin E blocked the 4-HPR-induced LC3 II expression (Fig. 5b, c); however, pre-incubation with myriocin did not prevent 4-HPR-elicited LC3 II expression (Fig. 5b, c). None of the inhibitors alone altered LC3 II expression (Fig. 5c).

4-HPR treatment elicits MAPK signaling

Under vehicle control conditions, phosphorylated (P) ERK was expressed in MIA PaCa-2 (Fig. 6a, *left*) and PANC-1 cells (Fig. 6a, *right*). Treatment with 4-HPR, however, decreased (P)ERK and increased non-phosphorylated ERK in MIA PaCa-2 cells (Fig. 6a). 4-HPR also leads to decreased (P)ERK in PANC-1 cells, and vitamin E or 3-MA pretreatment partially prevented the 4-HPR-induced decrease in (P)ERK (Fig. 6a). 4-HPR led to increased (P)p38 in both cell lines, and no change in non-phosphorylated p38 was observed (Fig. 6b). Vitamin E pretreatment partially blocked the 4-HPR-induced increase in (P)p38, while myriocin and 3-MA almost completely blocked the 4-HPR-induced increase in (P)p38 (Fig. 6b). Similarly, 4-HPR led to an increase in (P)JNK in both cell lines, and pretreatment with vitamin E, myriocin, and 3-MA prevented the 4-HPR-induced increases in (P)JNK (Fig. 6c).

Effect of inhibition of ROS and autophagy

Next, we tested whether blocking production of ROS or inhibiting autophagy would affect 4-HPR cytotoxicity. The bar graph in Fig. 7a and the corresponding histograms show that 4-HPR exposure produced a 3.0-fold increase in PI-positive stained cells over control at 72 h. Pretreatment with vitamin E and 3-MA, but not myriocin, provided limited protection from 4-HPR-induced cell death. Experiments measuring DNA synthesis at 24 h showed that 3-MA and 4-HPR decreased proliferation to similar degrees (53 and 49%, respectively), and the combination of 3-MA and 4-HPR led to a 78% reduction in DNA synthesis over control (Fig. 7b).

Discussion

In the present study, we show for the first time that clinically relevant concentrations of 4-HPR are growth

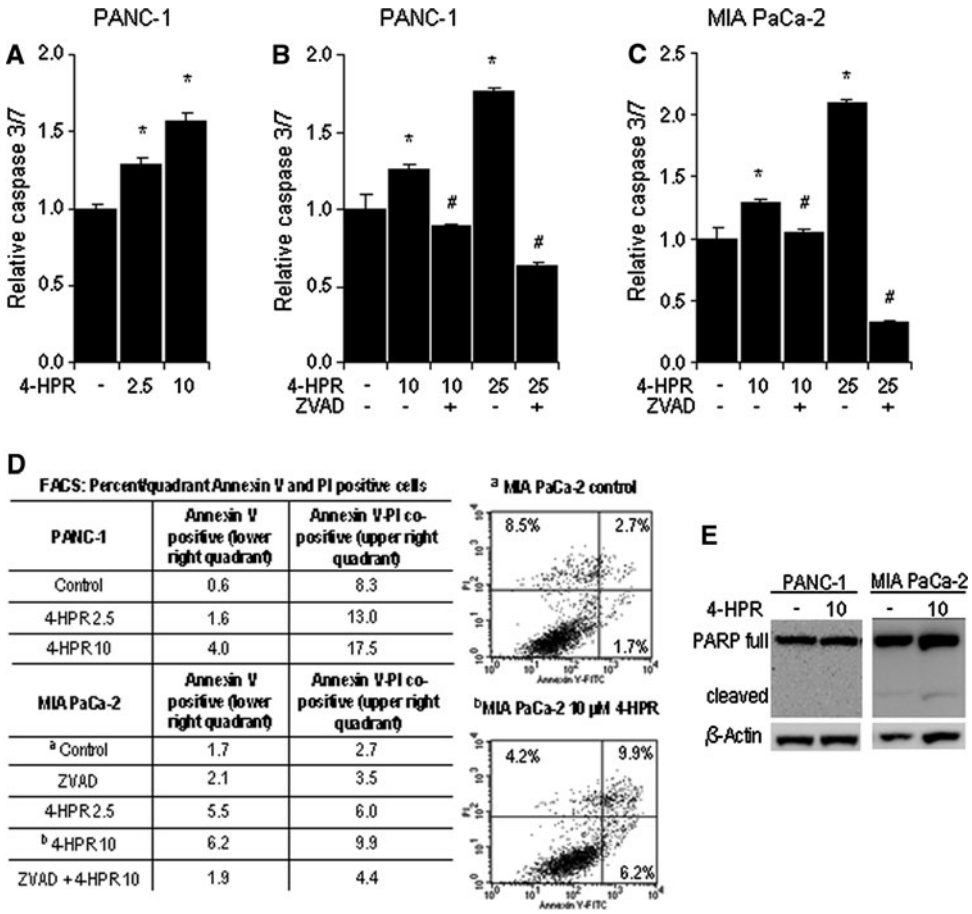

Fig. 4 Effect of 4-HPR on markers of apoptosis. (**a**–**c**) Caspase 3/7 activity was measured in (**a**) PANC-1 cells that were treated for 48 h ($n = 5$), and in (**b**) PANC-1 and **c** MIA PaCa-2 cells pretreated with 40 μM of the pan-caspase inhibitor Z-VAD-FMK (ZVAD) followed by vehicle(−) or 10 and 25 μM 4-HPR for 24 h ($n = 6$). Data represent fold change over control levels. One-way ANOVA with Tukey's *post hoc* analyses was preformed ($n = 3$). An asterisk denotes a significant difference between the control arm, and a number sign denotes a significant difference between the 4-HPR experimental arm, $P \leq 0.05$. (**d**) Flow cytometry of Annexin V/PI-positive cells. Cells pretreated with 40 μM ZVAD followed by exposure to vehicle (−) or 4-HPR (2.5 and 10 μM) for 48 h were co-stained with FITC-Annexin V (*x*-axis) and propidium iodide (PI) (*y*-axis). Data in the table show the percentage of cells per quadrant stained positive for Annexin V only and cells stained positive for both Annexin V and PI. Superscripts *a* and *b* in the table correspond to the dot plots shown to the right. (**e**) Western blot of full-length and cleaved PARP. Cells were treated for 48 h in the presence of vehicle (−) or 10 μM 4-HPR

inhibitory and cytotoxic to human pancreatic cancer cells. The mechanism of 4-HPR cytotoxicity is not fully understood; however, previous studies have documented the involvement of ceramide [36] among other factors. In the studies presented herein, 4-HPR led to an increase in the production of ceramide, which was derived from the de novo pathway and not the sphingomyelinase pathway (see Fig. 2). It should be noted that fumonisin B1 blocks ceramide synthase that converts sphinganine to dihydroceramide in the de novo pathway, as well as sphingosine to ceramide in the salvage pathway. Desipramine also has off-target effects by inhibiting ceramidase, the enzyme responsible for converting ceramide to sphingosine in the salvage pathway. Importantly, blocking the de novo pathway with myriocin or L-cycloserine decreased ceramide production, but blocking elements of the salvage pathway with GW4869 or desipramine did not decrease ceramide production. Unlike previous studies, inhibiting ceramide production with myriocin did not decrease 4-HPR cytotoxicity (see Fig. 7), nor did inhibition of sphingomyelinase with GW4869 and desipramine (data not shown), suggesting that ceramide does not contribute to 4-HPR cytotoxicity in pancreatic cancer cells. PANC-1 and MIA PaCa-2 cells metabolized over half of the ceramide generated in response to 4-HPR to glucosylceramide and sphingomyelin, classes of non-toxic sphingolipids (see Fig. 2). Upregulation of glucosylceramide synthase, the enzyme that converts ceramide to glucosylceramide, has been shown previously to play a role in resistance to ceramide-governed cytotoxicity [24] and thus may be a potential target for increasing sensitivity of pancreatic cancer cells to 4-HPR.

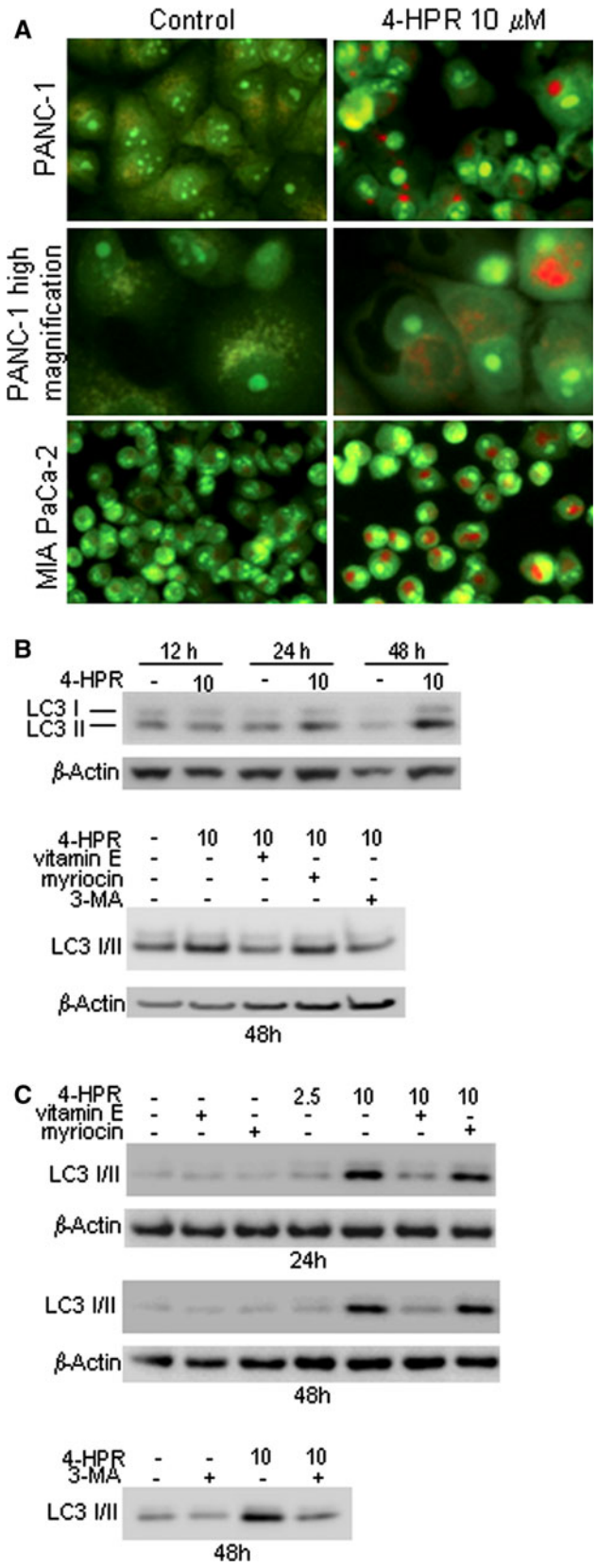

◀ **Fig. 5** Effect of 4-HPR on markers of autophagy. **a** Fluorescence microscopy of autophagic vesicles. Autophagasomes (*red/dark orange*) were visualized after a 48-h exposure to 4-HPR by staining cells with *acridine orange*. PANC-1 cells (*top and middle rows*) and MIA PaCa-2 cells (*bottom row*) were treated with 10 μM 4-HPR or vehicle (*Control*). **b**, **c** Western blot of LC3 I/II expression. **b** MIA PaCa-2 and **c** PANC-1 cells were pretreated with 250 μM vitamin E, 0.25 μM myriocin, 5 mM 3-MA, or vehicle (−) prior to incubation with 2.5 or 10 μM 4-HPR for 24 and 48 h

Elevated ROS has been shown to positively correlate with or directly lead to 4-HPR cytotoxicity in other cancer cell lines [16]. Furthermore, many ROS-generating agents have been shown to induce autophagy in transformed cells and in cancer cell lines but not in normal cells [1]. In the present study, 4-HPR elicited a sustained increase in ROS (see Fig. 3), and when ROS levels were abrogated by vitamin E, sensitivity to 4-HPR decreased (see Fig. 7). Additionally, in our system, blocking ROS led to decreased autophagy (see Fig. 5), suggesting that ROS plays a major role in 4-HPR autophagic cytotoxicity in these pancreatic cancer cell lines.

In data presented herein (see Fig. 6), 4-HPR led to a strong, sustained phosphorylation of JNK and p38 and decreased phosphorylation of ERK. In pancreatic cancer cells [15, 29, 40] and in clinical samples of pancreatic tumor tissue [17, 18, 38], ERK is aberrantly and constitutively upregulated. In some studies, ERK aids in pancreatic cell proliferation [15, 18] and may be negatively regulated by p38 [9]. Activated JNK has been shown to phosphorylate Bcl-2, leading to its dissociation from beclin 1 to initiate autophagy [27, 32], and ceramide has been shown to activate JNK and cause the dissociation of Bcl-2 and beclin-1 [7, 42]. Ceramide was also shown to be required for induction of autophagy in human cancer cell lines [27]. In the studies presented herein, inhibiting the increase in de novo ceramide levels with myriocin decreased 4-HPR-induced expression of phosphorylated JNK but did not decrease 4-HPR cytotoxicity (see Figs. 6 and 7), suggesting that ceramide does not contribute to 4-HPR cytotoxicity in pancreatic cancer cells. 4-HPR also led to a strong, sustained phosphorylation of JNK and p38, which was prevented by de novo ceramide inhibitor myriocin, or autophagy inhibitor 3-MA. These data suggest either that the sphingolipid and autophagic pathways induce activity of the MAPK enzymes or that the inhibitors have off-target effects. Future studies will be required to elucidate the relative influence of the individual MAPK members on 4-HPR-induced cytotoxicity.

In the present study, indications of apoptosis, albeit weak, included caspase 3/7 activity and Annexin V binding.

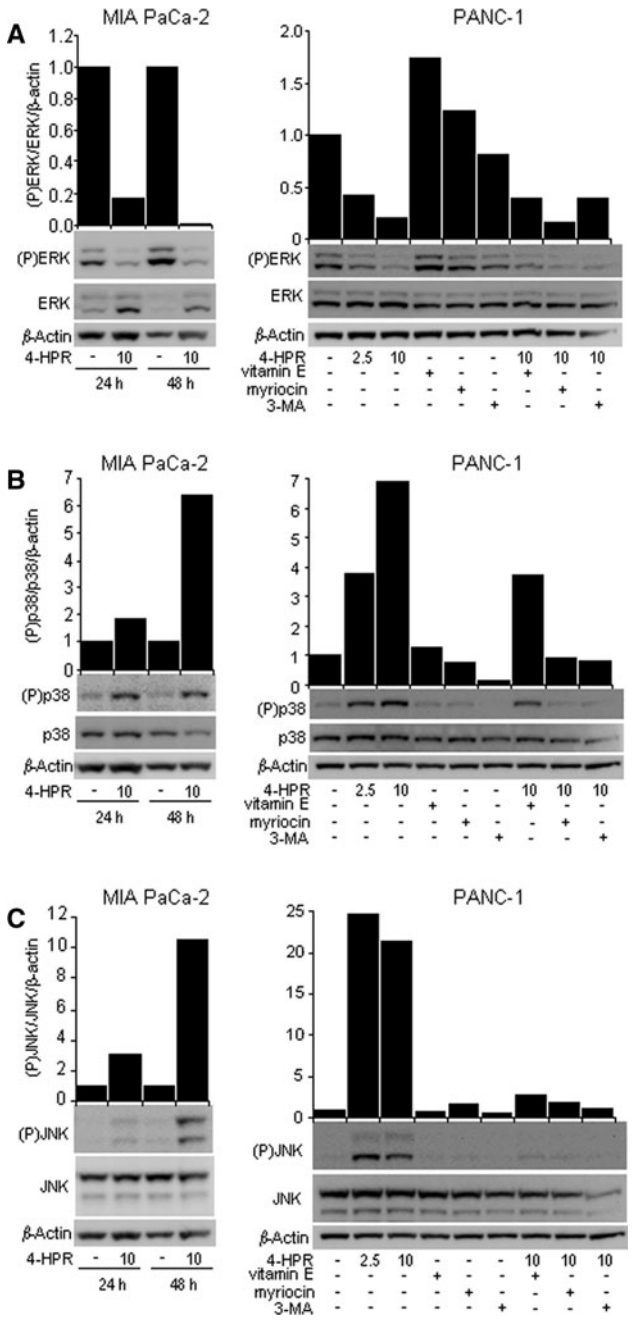

Fig. 6 Effect of 4-HPR on the phosphorylation of the MAPK family of kinases. **a–c** Western blot of MAPKs. Expression of phosphorylated and non-phosphorylated isoforms of (**a**) ERK(p44/42), **b** p38, and **c** SAPK/JNK (p54/46). MIA PaCa-2 cells (*left column*) were exposed to vehicle (−) or 10 μM 4-HPR for 24 or 48 h. PANC-1 cells (*right column*) were pretreated with 250 μM vitamin E, 0.25 μM myriocin, 5 mM 3-MA, or vehicle prior to addition of 10 μM 4 HPR for 48 h. *Blots* are representative of repeated experiments, and densitometry plots display the phosphorylated protein/non-phosphorylated protein/ *β*-actin, normalized to control

Although membrane blebbing and plasma membrane phosphatidylserine presentation is an ATP-dependent process that has also been shown to occur during autophagy [19], a pan-caspase inhibitor was sufficient to decrease the percentage of FITC-Annexin V-positive cells nearly to control levels (see Fig. 4), suggesting that 4-HPR induces canonical apoptosis. The apoptosis was likely caspase dependent, as there was a slight increase in caspase 3/7 activity and no DNA laddering or upregulation of AIF, a caspase-independent protein. Hallmarks of autophagy were also expressed in response to 4-HPR treatment. The autophagy inhibitor 3-MA decreased basal PANC-1 cell proliferation, at levels similar to 4-HPR. This suggested to us that autophagy is required for normal pancreatic cancer cell viability. However, 3-MA also decreased cell death initiated by 4-HPR as measured by propidium iodide staining, suggesting that autophagy is also the route by which 4-HPR provokes cytotoxicity.

There are several possible explanations for the co-occurrence of markers for autophagy and apoptosis, and one explanation is that cancer cells are dose sensitive. Data presented in Fig. 4 show increased caspase 3/7 activity and an increase in FITC-Annexin V-positive cells at higher compared with lower concentrations of 4-HPR. A similar example was shown in HL-60 leukemia cell response to tamoxifen, which induced autophagy at low concentrations, apoptosis at medium concentrations, and necrosis at high concentrations [5]. Another explanation is that caspase 3/7 activation is either integral to the execution of autophagy-mediated cell death or that autophagy precedes caspase activation and cell death [4]. A variety of drugs have been shown to coordinately activate autophagy and apoptosis in leukemia [28, 41], Kaposi's sarcoma [3], and in prostate cancer cells [39]. There are many genes that are shared between autophagy and apoptosis, and cross talk has been observed [11, 23, 27, 28].

Another probable reason for the co-occurrence of autophagy and apoptosis markers is that the dominant response to 4-HPR is apoptosis in some cells and autophagy in other cells. Pancreatic tumors are highly heterogeneic, i.e., cells from the same tumor will express different genotypes [17]. In a recent study, examination of individual cancer cells showed evidence of autophagy in some cells and apoptosis in other cells, but not concurrently in the same cell in response to 4-HPR challenge [22]. Regardless, in this study, 4-HPR was cytotoxic to both MIA PaCa-2 and PANC-1, whether by induction of autophagy or apoptosis, and future studies will be required to fully elucidate the mechanism of cell death.

In summary, we have shown in human pancreatic cancer cells that 4-HPR increased ROS, elicited de novo ceramide generation, increased the phosphorylation of JNK and p38, and decreased ERK phosphorylation. Importantly, we show for the first time that clinically relevant concentrations of 4-HPR are cytotoxic to PANC-1 and MIA PaCa-2 pancreatic cancer cells. Drug combinations to further amplify the

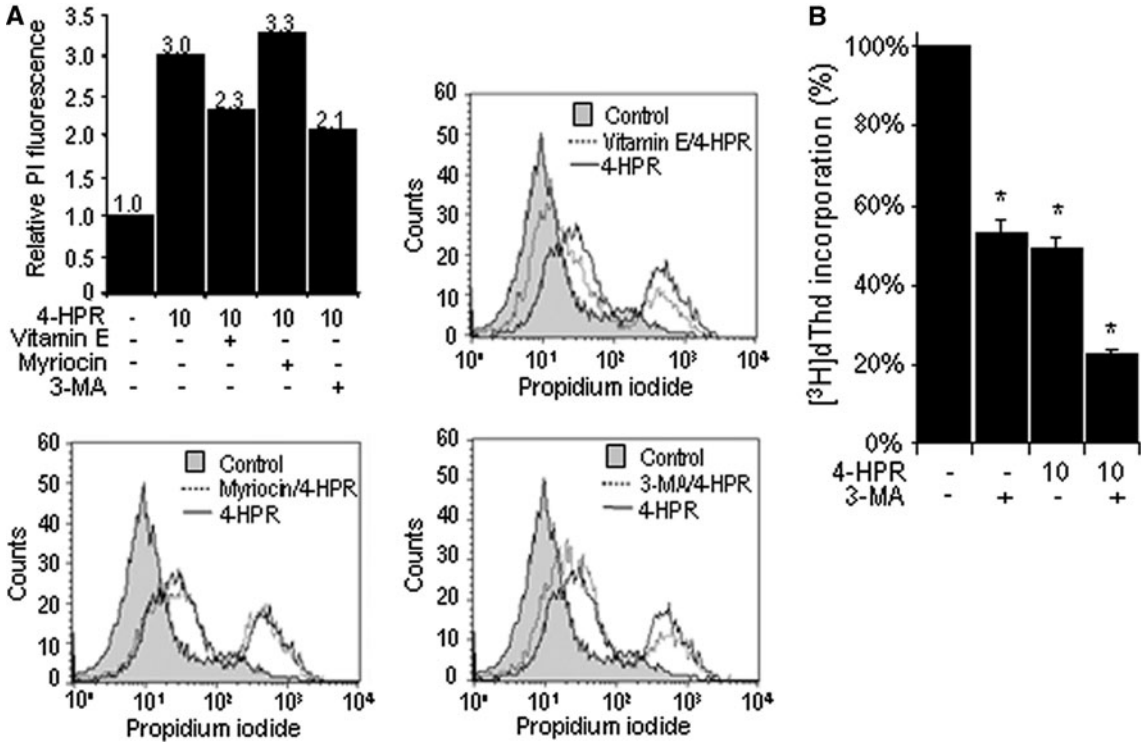

Fig. 7 Effect of vitamin E, myriocin, and 3-MA on PANC-1 sensitivity to 4-HPR. **a** Cell death analyzed by flow cytometry. Cells were pretreated with vehicle (−),0.25 μM myriocin, 250 μM vitamin E, or 5 mM 3-MA, followed by 10 μM 4-HPR for 72 h. Cells were then stained with propidium iodide (PI) and analyzed by flow cytometry. *Bar graph* shows fold increase in mean PI fluorescence in treated cells compared with control. The corresponding histograms show PI distribution in control cells (*gray area under curve*), 4-HPR-treated cells (*solid line*), and cells pretreated before 4-HPR addition (*broken line*). **b** DNA synthesis. PANC-1 cells were pretreated with 5 mM 3-MA or vehicle (−), followed by a 24-h treatment with vehicle (−) or 10 μM 4-HPR. [^{3}H]Thymidine (dThd) was added to wells for 1 h, and radioactivity was measured as detailed in "Materials and methods". Data represent fold change over control levels. One-way ANOVA with Tukey's *post hoc* analyses was preformed ($n = 3$). An *asterisk* denotes a significant difference between the control arm, and a number sign denotes a significant difference between the 4-HPR experimental arm, $P \leq 0.05$

cytotoxicity of 4-HPR, targeting strategies, and/or new drug formulations will likely be a pertinent endeavor.

Acknowledgements This work was supported by USPHS grants from the National Cancer Institute (CA143755) and the National Institute of General Medical Sciences (GM77391).

Conflict of interest None.

References

1. Azad MB, Chen Y, Gibson SB (2009) Regulation of autophagy by reactive oxygen species (ROS): implications for cancer progression and treatment. Antioxid Redox Signal 11:777–790
2. Barna G, Sebestyen A, Weischede S, Petak I, Mihalik R, Formelli F, Kopper L (2005) Different ways to induce apoptosis by fenretinide and all-trans-retinoic acid in human B lymphoma cells. Anticancer Res 25:4179–4185
3. Basciani S, Vona R, Matarrese P, Ascione B, Mariani S, Cauda R, Gnessi L, Malorni W, Straface E, Lucia MB (2007) Imatinib interferes with survival of multi drug resistant Kaposi's sarcoma cells. FEBS Lett 581:5897–5903
4. Berry DL, Baehrecke EH (2007) Growth arrest and autophagy are required for salivary gland cell degradation in Drosophila. Cell 131:1137–1148
5. Bursch W, Karwan A, Mayer M, Dornetshuber J, Frohwein U, Schulte-Hermann R, Fazi B, Di Sano F, Piredda L, Piacentini M, Petrovski G, Fesus L, Gerner C (2008) Cell death and autophagy: cytokines, drugs, and nutritional factors. Toxicology 254:147–157
6. Cheung E, Pinski J, Dorff T, Groshen S, Quinn DI, Reynolds CP, Maurer BJ, Lara PN Jr, Tsao-Wei DD, Twardowski P, Chatta G, McNamara M, Gandara DR (2009) Oral fenretinide in biochemically recurrent prostate cancer: a California cancer consortium phase II trial. Clin Genitourin Cancer 7:43–50
7. Daido S, Kanzawa T, Yamamoto A, Takeuchi H, Kondo Y, Kondo S (2004) Pivotal role of the cell death factor BNIP3 in ceramide-induced autophagic cell death in malignant glioma cells. Cancer Res 64:4286–4293
8. Decensi A, Robertson C, Guerrieri-Gonzaga A, Serrano D, Cazzaniga M, Mora S, Gulisano M, Johansson H, Galimberti V, Cassano E, Moroni SM, Formelli F, Lien EA, Pelosi G, Johnson KA, Bonanni B (2009) Randomized double-blind 2 × 2 trial of low-dose tamoxifen and fenretinide for breast cancer prevention in high-risk premenopausal women. J Clin Oncol 27:3749–3756
9. Ding XZ, Adrian TE (2001) MEK/ERK-mediated proliferation is negatively regulated by P38 map kinase in the human pancreatic cancer cell line, PANC-1. Biochem Biophys Res Commun 282:447–453

10. Dorr RT, Raymond MA, Landowski TH, Roman NO, Fukushima S (2005) Induction of apoptosis and cell cycle arrest by imexon in human pancreatic cancer cell lines. Int J Gastrointest Cancer 36:15–28
11. Eisenberg-Lerner A, Bialik S, Simon HU, Kimchi A (2009) Life and death partners: apoptosis, autophagy and the cross-talk between them. Cell Death Differ 16:966–975
12. Fazi B, Bursch W, Fimia GM, Nardacci R, Piacentini M, Di Sano F, Piredda L (2008) Fenretinide induces autophagic cell death in caspase-defective breast cancer cells. Autophagy 4:435–441
13. Formelli F, Cavadini E, Appierto V, Tiberio P, Grigolato R, Chiesa F, Tradati N, Persiani S (2009) Comment re: continuous rather than intermittent administration of fenretinide in leukoplakia. Cancer Prev Res 2:281; author reply 281 (Phila Pa)
14. Garaventa A, Luksch R, Lo Piccolo MS, Cavadini E, Montaldo PG, Pizzitola MR, Boni L, Ponzoni M, Decensi A, De Bernardi B, Bellani FF, Formelli F (2003) Phase I trial and pharmacokinetics of fenretinide in children with neuroblastoma. Clin Cancer Res 9:2032–2039
15. Gysin S, Lee SH, Dean NM, McMahon M (2005) Pharmacologic inhibition of RAF– > MEK– > ERK signaling elicits pancreatic cancer cell cycle arrest through induced expression of p27Kip1. Cancer Res 65:4870–4880
16. Hail N Jr, Kim HJ, Lotan R (2006) Mechanisms of fenretinide-induced apoptosis. Apoptosis 11:1677–1694
17. Hezel AF, Kimmelman AC, Stanger BZ, Bardeesy N, Depinho RA (2006) Genetics and biology of pancreatic ductal adenocarcinoma. Genes Dev 20:1218–1249
18. Hirano T, Shino Y, Saito T, Komoda F, Okutomi Y, Takeda A, Ishihara T, Yamaguchi T, Saisho H, Shirasawa H (2002) Dominant negative MEKK1 inhibits survival of pancreatic cancer cells. Oncogene 21:5923–5928
19. Inbal B, Bialik S, Sabanay I, Shani G, Kimchi A (2002) DAP kinase and DRP-1 mediate membrane blebbing and the formation of autophagic vesicles during programmed cell death. J Cell Biol 157:455–468
20. Kalli KR, Devine KE, Cabot MC, Arnt CR, Heldebrant MP, Svingen PA, Erlichman C, Hartmann LC, Conover CA, Kaufmann SH (2003) Heterogeneous role of caspase-8 in fenretinide-induced apoptosis in epithelial ovarian carcinoma cell lines. Mol Pharmacol 64:1434–1443
21. Kraveka JM, Li L, Szulc ZM, Bielawski J, Ogretmen B, Hannun YA, Obeid LM, Bielawska A (2007) Involvement of dihydroceramide desaturase in cell cycle progression in human neuroblastoma cells. J Biol Chem 282:16718–16728
22. Lai WL, Wong NS (2008) The PERK/eIF2 alpha signaling pathway of Unfolded Protein Response is essential for N-(4-hydroxyphenyl)retinamide (4HPR)-induced cytotoxicity in cancer cells. Exp Cell Res 314:1667–1682
23. Levine B, Sinha S, Kroemer G (2008) Bcl-2 family members: dual regulators of apoptosis and autophagy. Autophagy 4:600–606
24. Liu YY, Yu JY, Yin D, Patwardhan GA, Gupta V, Hirabayashi Y, Holleran WM, Giuliano AE, Jazwinski SM, Gouaze-Andersson V, Consoli DP, Cabot MC (2008) A role for ceramide in driving cancer cell resistance to doxorubicin. FASEB J 22:2541–2551
25. Maurer BJ, Metelitsa LS, Seeger RC, Cabot MC, Reynolds CP (1999) Increase of ceramide and induction of mixed apoptosis/necrosis by N-(4-hydroxyphenyl)- retinamide in neuroblastoma cell lines. J Natl Cancer Inst 91:1138–1146
26. Modrak DE, Leon E, Goldenberg DM, Gold DV (2009) Ceramide regulates gemcitabine-induced senescence and apoptosis in human pancreatic cancer cell lines. Mol Cancer Res 7:890–896
27. Pattingre S, Bauvy C, Carpentier S, Levade T, Levine B, Codogno P (2009) Role of JNK1-dependent Bcl-2 phosphorylation in ceramide-induced macroautophagy. J Biol Chem 284:2719–2728
28. Qian W, Liu J, Jin J, Ni W, Xu W (2007) Arsenic trioxide induces not only apoptosis but also autophagic cell death in leukemia cell lines via up-regulation of Beclin-1. Leuk Res 31:329–339
29. Sawai H, Okada Y, Funahashi H, Matsuo Y, Takahashi H, Takeyama H, Manabe T (2005) Activation of focal adhesion kinase enhances the adhesion and invasion of pancreatic cancer cells via extracellular signal-regulated kinase-1/2 signaling pathway activation. Mol Cancer 4:37
30. Senchenkov A, Litvak DA, Cabot MC (2001) Targeting ceramide metabolism–a strategy for overcoming drug resistance. J Natl Cancer Inst 93:347–357
31. Sun SY, Li W, Yue P, Lippman SM, Hong WK, Lotan R (1999) Mediation of N-(4-hydoxyphenyl)retinamide-induced apoptosis in human cancer cells by different mechanisms. Cancer Res 59:2493–2498
32. Takacs-Vellai K, Vellai T, Puoti A, Passannante M, Wicky C, Streit A, Kovacs AL, Muller F (2005) Inactivation of the autophagy gene bec-1 triggers apoptotic cell death in C. elegans. Curr Biol 15:1513–1517
33. Tiwari M, Bajpai VK, Sahasrabuddhe AA, Kumar A, Sinha RA, Behari S, Godbole MM (2008) Inhibition of N-(4-hydroxyphenyl)retinamide-induced autophagy at a lower dose enhances cell death in malignant glioma cells. Carcinogenesis 29:600–609
34. Villablanca JG, Krailo MD, Ames MM, Reid JM, Reaman GH, Reynolds CP (2006) Phase I trial of oral fenretinide in children with high-risk solid tumors: a report from the Children's Oncology Group (CCG 09709). J Clin Oncol 24:3423–3430
35. Wang H, Maurer BJ, Liu YY, Wang E, Allegood JC, Kelly S, Symolon H, Liu Y, Merrill AH Jr, Gouaze-Andersson V, Yu JY, Giuliano AE, Cabot MC (2008) N-(4-Hydroxyphenyl)retinamide increases dihydroceramide and synergizes with dimethylsphingosine to enhance cancer cell killing. Mol Cancer Ther 7:2967–2976
36. Wang H, Maurer BJ, Reynolds CP, Cabot MC (2001) N-(4-hydroxyphenyl)retinamide elevates ceramide in neuroblastoma cell lines by coordinate activation of serine palmitoyltransferase and ceramide synthase. Cancer Res 61:5102–5105
37. William WN Jr, Lee JJ, Lippman SM, Martin JW, Chakravarti N, Tran HT, Sabichi AL, Kim ES, Feng L, Lotan R, Papadimitrakopoulou VA (2009) High-dose fenretinide in oral leukoplakia. Cancer Prev Res (Phila Pa) 2:22–26
38. Yamamoto S, Tomita Y, Hoshida Y, Morooka T, Nagano H, Dono K, Umeshita K, Sakon M, Ishikawa O, Ohigashi H, Nakamori S, Monden M, Aozasa K (2004) Prognostic significance of activated Akt expression in pancreatic ductal adenocarcinoma. Clin Cancer Res 10:2846–2850
39. Yang W, Monroe J, Zhang Y, George D, Bremer E, Li H (2006) Proteasome inhibition induces both pro- and anti-cell death pathways in prostate cancer cells. Cancer Lett 243:217–227
40. Yokoi K, Fidler IJ (2004) Hypoxia increases resistance of human pancreatic cancer cells to apoptosis induced by gemcitabine. Clin Cancer Res 10:2299–2306
41. Yokoyama T, Miyazawa K, Naito M, Toyotake J, Tauchi T, Itoh M, Yuo A, Hayashi Y, Georgescu MM, Kondo Y, Kondo S, Ohyashiki K (2008) Vitamin K2 induces autophagy and apoptosis simultaneously in leukemia cells. Autophagy 4:629–640
42. Zhang H, Bosch-Marce M, Shimoda LA, Tan YS, Baek JH, Wesley JB, Gonzalez FJ, Semenza GL (2008) Mitochondrial autophagy is an HIF-1-dependent adaptive metabolic response to hypoxia. J Biol Chem 283:10892–10903